HOLOGRAPHIC AND SPECKLE METHODS

A. Albertazzi G. Jr
Department of Mechanical Engineering, Universidade Federal de Santa Catarina, Brazil

M. R. Viotti
Optical Metrology Division, Photonita Ltda, Brazil

Keywords: Experimental mechanics, optical metrology, holography, holographic interferometry, digital holography, speckle, speckle correlation, speckle interferometry, DSPI, ESPI.

Contents

Bibliography
Biographical Sketches

Summary

Two important full filed optical techniques widely used in experimental mechanic applications are presented in this topic: *holography* and *speckle methods*. Holography is well known for generating three dimensional images. In addition, holography can also be used for very accurately compare three dimensional images of a same object before and after a deformation is applied. That is the basis of a full filed optical measurement technique named *holographic interferometry*. The principles, equations and few applications are presented here. A more recent development named *digital holography*, which intensively uses image and computer processing, is also presented and discussed. Laser light reflected by a rough surface produces a curious effect known as *speckle*, which is like an optical granularity visible on the surface. The speckle effect can be used for measurements. Two images of the same object, after and before loading, can be very accurately compared if the speckle effect is conveniently used. That is the basis for a technique named *digital speckle correlation*, which will be discussed here. The optical superposition of two speckle patterns produces a new effect named *speckle interferometry*, which brings new possibilities for high precision measurements in the experimental mechanics field. The principles, main techniques, configurations and applications of *digital speckle pattern interferometry* are progressively discussed in this text. To make the text comprehensive for new readers, a brief introduction of light waves and wave mathematics is also included as an introductory topic.

1. Holographic Methods

Holography is well known for the ability to produce three dimensional images. Holographic images are used in arts as well as in commercial applications such as in souvenirs or credit cards. Three dimensional images are produced because holography is capable to record and reconstruct light waves. This property makes possible to accurately compare two light waves coming from a same object before and after deformation through *holographic interferometry*. The two light waves interfere and the resulting optical effect is the development of fringe patterns that encode information about the deformations applied to the object. By appropriated processing, the deformations, strains and stresses fields can be computed for the visible area of a loaded object. This full field information is a very important tool for experimental mechanics applications.

This item starts with an introduction about light waves and its mathematical representations. The principles and mathematics behind the recording and reconstruction of light waves by holography using high resolution films is presented. After that, the basic principles about techniques of holographic interferometry are discussed as well as a few applications are given. Finally, the fundamentals and applications of digital holography close this item.

1.2. Light Waves

Visible light is an electromagnetic radiation that can be seen by the human eye. It is composed by elementary particles called *photons*. However, light is also a wave. The modern theory that explains the nature of light includes the notion of wave-particle duality described by Einstein. In this item only the wave nature of light will be explored.

1.1.1. Wave mathematics

In the simplest form, the electric field of a light wave that propagates in the positive direction of the z axis can be described by Eq. (1):

$$E(z,t) = E_0 \cos(kz - \omega t + \theta) \qquad (1)$$

Note that a light wave propagates in space (z) and in time (t), as illustrates Figure 1. For a given instant t_0 the electric field changes periodically with space along the z axis. The spatial period λ is known as the *wavelength*. For a given point fixed in space z_0 the electric field also changes periodically with time. The time period T is represented in the figure. The quantity E_0 is the electric field amplitude, represented as the amplitude of the cosine wave.

The quantity inside of the parenthesis of Eq. (1) is the *phase* of the wave. Note that the phase changes with time and space. θ is the initial phase value at the time and space origin ($t = 0$ and $z = 0$). The space coefficient k is known as the *wave number*, and is related with the light wavelength λ by Eq. (2). The wavelength of visible light is a very small quantity, and is related with the color perception that human beings have. Violet light has a shorter wavelength of about 390 nm and red light reaches up to 760 nm.

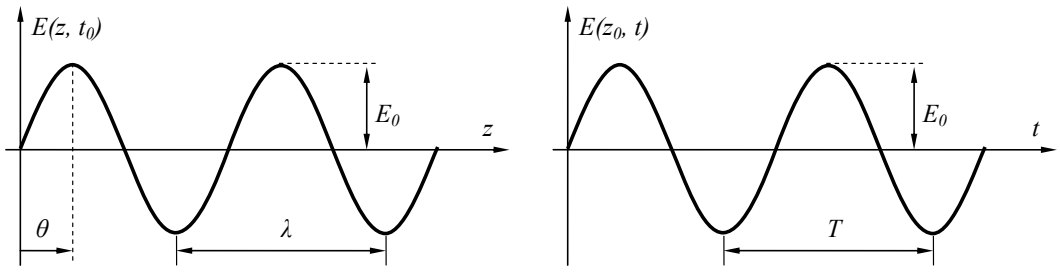

Figure 1. Light propagation in space and time. Left: a snap shot of the light propagation for a fixed instant t_0. Right: light propagation as a function of time for a fixed point at z_0.

$$k = \frac{2\pi}{\lambda} \qquad (2)$$

The time coefficient ω is the angular frequency of the light and is related to the frequency v by Eq. (3). The frequency is associated to the time period T by $v = 1/T$ Light frequency is very high, ranging from 3.84×10^{14} Hz for red light until 7.69×10^{14} Hz for violet light. It is far beyond the capability to be detected by the light sensors available today. The product λv is constant and equal to c, the velocity of light.

$$\omega = 2\pi v \tag{3}$$

Sometimes the trigonometric form of Eq. (1) is very convenient. Sometimes, it makes some calculations very hard to be accomplished. For such cases, the work can be considerably easier with complex notation using the *Euler's formula*:

$$e^{i\phi} = \cos\phi + i\sin\phi \tag{4}$$

If only the real part of Eq. (4) is considered, Eq. (1) can be rewritten as:

$$E(z,t) = \mathrm{Re}[E_0\, e^{i(kz-\omega t+\theta)}] \tag{5}$$

This approach is so usual that frequently the Re indication is not written, and Eq. (1) is written as Eq. (6). However, it is implicitly understood that only the real part of Eq. (6) has a physical meaning.

$$E(z,t) = E_0\, e^{i(kz-\omega t+\theta)} \tag{6}$$

Equations (1) and (6) represent a wave propagating along the z axis. For a given time t_0 the phase value depends only of z. It means the all points that lay on the plane $z = z_1$ have the same phase value. *Wavefront* is the name given for the surface of a wave that has a constant phase value at a given time. The wavefronts are perpendicular to the propagation direction. Therefore, Eqs. (1) or (6) refer to a wave with a plane wavefront. In the real world there are not only light waves with plane wavefronts. Equation (6) can be generalized as in Eq. (7) to describe waves with any arbitrary wavefront by introducing the dot product between the spatial vector $\mathbf{r} = (x, y, z)$ and the wave vector $\boldsymbol{\kappa} = f(\mathbf{r})$. The wave propagates in the direction of the wave vector $\boldsymbol{\kappa}$.

$$E(\mathbf{r},t) = E_0 e^{i(\mathbf{k}\cdot} \tag{6}$$

The response of the eyes and any artificial sensors to light is proportional to the light *intensity*, which is the energy flux throughout an area per time. The intensity is proportional to the square of the amplitude of the electric field:

$$I = \left|E_0\right|^2 = E_0 E_0^* \tag{7}$$

where E_0^* is the complex conjugate of E_0.

1.1.2. Interference

The superposition of two or more light waves produces the physical effect known as *interference*. The resulting amplitudes, phases and intensities come from the interaction between them. Though interference can occur between waves with different frequencies, this text will focus only on interference between waves with same frequencies. The interference effect is only stable and visible if the light waves are *coherent*, what means that they are correlated in such a way that the relative phase differences between the waves are stable. That is possible to be reached only if the light waves that interfere come from the same light source and the light path differences are not longer than the *coherence length* of the light source. White light sources have coherence lengths in the range of only few micrometers while laser sources can reach few millimeters to tens or hundreds of meters.

Lets E_{A} and E_{B} be two coherent light waves with same frequency and arbitrary wavefronts. In this case $\omega_{\mathrm{A}} = \omega_{\mathrm{B}} = \omega$. Equations for E_{A} and E_{B} are given in Eq. (8):

$$\begin{aligned} E_{\mathrm{A}}(\mathbf{r},t) &= E_{0\mathrm{A}}\, e^{i(\mathbf{k}_{\mathrm{A}} \cdot \quad ,)} \\ E_{\mathrm{B}}(\mathbf{r},t) &= E_{0\mathrm{B}}\, e^{i(\mathbf{k}_{\mathrm{B}} \cdot \quad ;)} \end{aligned} \tag{8}$$

The resulting interference can be computed by simple addition of both equations:

$$E(\mathbf{r},t) = E_{\mathrm{A}}(\mathbf{r},t) + E_{\mathrm{B}}(\mathbf{r},t) \tag{9}$$

The resulting intensity is computed by

$$\begin{aligned} I(\mathbf{r},t) &= [E_{\mathrm{A}}(\mathbf{r},t) + E_{\mathrm{B}}(\mathbf{r},t)][E_{\mathrm{A}}^{*}(\mathbf{r},t) + E_{\mathrm{B}}^{*}(\mathbf{r},t)] \\ &= [E_{0\mathrm{A}}\, e^{i(\mathbf{k}_{\mathrm{A}}\cdot\mathbf{r}-\omega t+\theta_{\mathrm{A}})} + E_{0\mathrm{B}}\, e^{i(\mathbf{k}_{\mathrm{B}}\cdot\mathbf{r}-\omega t+\theta_{\mathrm{B}})}][E_{0\mathrm{A}}\, e^{-i(\mathbf{k}_{\mathrm{A}}\cdot\mathbf{r}-\omega t+\theta_{\mathrm{A}})} \\ &+ E_{0\mathrm{B}}\, e^{-i(\mathbf{k}_{\mathrm{B}}\cdot\mathbf{r}-\omega t+\theta_{\mathrm{B}})}] \\ &= E_{0\mathrm{A}}^{2} + E_{0\mathrm{B}}^{2} + E_{0\mathrm{A}}E_{0\mathrm{B}}[e^{i(\mathbf{k}_{\mathrm{A}}\cdot\mathbf{r}+\mathbf{k}_{\mathrm{B}}\cdot\mathbf{r}+\theta_{\mathrm{A}}-\theta_{\mathrm{B}})} + e^{-i(\mathbf{k}_{\mathrm{A}}\cdot\mathbf{r}+\mathbf{k}_{\mathrm{B}}\cdot\mathbf{r}+\theta_{\mathrm{A}}-\theta_{\mathrm{B}})}] \\ &= E_{0\mathrm{A}}^{2} + E_{0\mathrm{B}}^{2} + 2E_{0\mathrm{A}}E_{0\mathrm{B}}\cos[(\boldsymbol{\kappa}_{\mathrm{A}}\cdot\mathbf{r}+\theta_{\mathrm{A}}) - (\boldsymbol{\kappa}_{\mathrm{B}}\cdot\mathbf{r}+\theta_{\mathrm{B}})] \end{aligned}$$

That can finally be written in terms of intensity as:

$$I(\mathbf{r},t) = I_{\mathrm{A}} + I_{\mathrm{B}} + 2\sqrt{I_{\mathrm{A}}I_{\mathrm{B}}}\cos[(\boldsymbol{\kappa}_{\mathrm{A}}\cdot\mathbf{r}+\theta_{\mathrm{A}}) - (\boldsymbol{\kappa}_{\mathrm{B}}\cdot\mathbf{r}+\theta_{\mathrm{B}})] \tag{10}$$

Note that the third term of the resulting intensity is a function of the non temporal term of the phase difference between E_{A} and E_{B}. Since the cosine function varies from -1 to

1, the resulting intensity has regions with local minima and maxima that are not time-dependent if both waves are stable in time.

1.1.3. Interference Fringes

From the macroscopic point of view the local maxima and minima of Eq. (10) produces lighter or brighter regions on the interference patterns known as *interference fringes*. Figure 2 shows a graphical representation of the interference fringes produced by superposition of two plane waves with different propagation angles. Note a fringe patterns formed by a set of horizontal dark and bright fringes in the overleaping region. If both light waves that interfere have the same frequency and are stable, the loci of the fringes are constant in time.

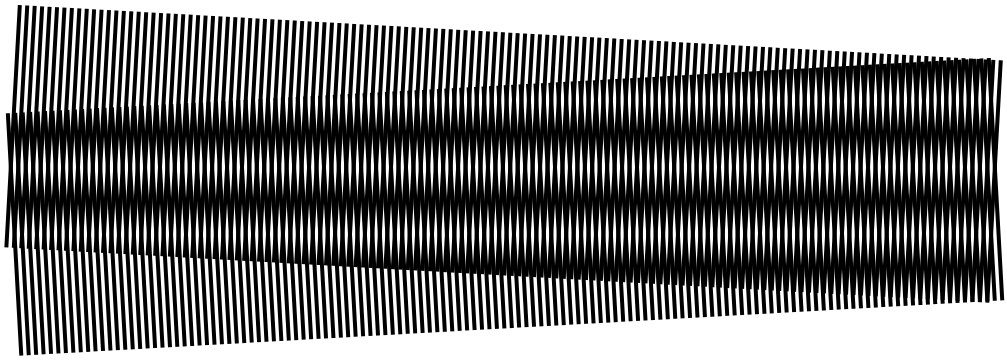

Figure 2. Interference fringes between two plane waves.

Bright fringes are the loci where the argument of the cosine function of Eq. (10) is equal to one. It depends on the phase difference between the light waves that interferes, that is only a function of space $\mathbf{r} = (x, y, z)$. The light intensity in a given point is also a periodic function of time. However, since the frequency range is at the order of 10^{14} Hz, it can not be detected. Consequently, for practical proposes, the time dependency of Eq. (10) can be neglected, and it can be rewritten in a simpler form as:

$$I(\mathbf{r}) = a(\mathbf{r}) + b(\mathbf{r})\cos[\varphi(\mathbf{r})] \qquad (11)$$

where $\varphi(\mathbf{r})$ is the phase difference between both interfering waves. $a(\mathbf{r}) = I_{\mathrm{A}} + I_{\mathrm{B}}$ is called as the *background intensity*. $b(\mathbf{r}) = 2\sqrt{I_{\mathrm{A}} I_{\mathrm{B}}}$ is known as the *modulation* coefficient and is related to the fringe contrast, or fringe *visibility*. Higher values of $b(\mathbf{r})$ produce better fringe visibility.

1.1.4. Phase Extraction

Frequently the phase difference $\varphi(\mathbf{r})$ between two waves encodes information that an experimentalist is interested to retrieve. Usually an image of the fringe patter is acquired and digitally processed. In this case, it is more convenient to describe the interference fringe equation as a function of the image coordinates *x* and *y* as follows:

$$I(x,y) = a(x,y) + b(x,y)\cos[\varphi(x,y)] \quad (12)$$

There are several approaches to retrieve $\varphi(x, y)$, but this is not an easy task. The main difficulty comes from the ambiguity brought by the cosine function. There are an infinite number of angles that have a same cosine value. They are $\cos(\alpha) = \cos(-\alpha) = \cos(\alpha + 2\pi n) = \cos(-\alpha + 2\pi n)$ for any integer n. There is no explicit indication in a single fringe pattern about with one is the correct angle value. For this reason, additional information is needed.

The fringes of an interference fringe pattern can be thought as contour lines of a relief where the heights are the phase values. Therefore, there are always a contour number related to each fringe. Although the fringe lines can be highlighted by an image processing techniques known as *fringe skeletonization*, unfortunately nature does not write a label with fringe numbering in the fringe patterns. In simpler cases it is not so difficult to follow certain rules for fringe numbering in continuous surfaces either manually or automatically. However, that is not the general case.

There are several other approaches for retrieving phase information. For example: temporal heterodyning methods, spatial heterodyning methods and spatial Fourier transform methods. They will not be discussed here. The focus will go only to a class of method known as *phase stepping*.

The idea of phase stepping is to artificially introduce a known and controlled phase shift between the light waves that interfere. That can be done, for instance, by slightly modifying the optical path length of one of the waves. For example, a mirror can be moved by a small amount by a piezo electric translator. An increment in the optical path length of only $\pi/4$ will produce a relative phase shift of $\pi/2$ rad. Usually few fringe patterns, with different well known phase shifts, are digitally recorded, combined and processed. One of the simplest and more popular algorithms for retrieving the phase value uses a set of four $\pi/2$ phase shifted fringe patterns, as is shown in Figure 3. By introducing 0, $\pi/2$, $\pi/2$ and $3\pi/2$ phase shifts in Eq. (12), four equations result:

$$\begin{aligned}
I_0(x,y) &= a(x,y) + b(x,y)\cos[\varphi(x,y) + 0] &&= a(x,y) + b(x,y)\cos[\varphi(x,y)] \\
I_{\pi/2}(x,y) &= a(x,y) + b(x,y)\cos[\varphi(x,y) + \pi/2] &&= a(x,y) - b(x,y)\sin[\varphi(x,y)] \\
I_{\pi}(x,y) &= a(x,y) + b(x,y)\cos[\varphi(x,y) + \pi] &&= a(x,y) - b(x,y)\cos[\varphi(x,y)] \\
I_{3\pi/2}(x,y) &= a(x,y) + b(x,y)\cos[\varphi(x,y) + 3\pi/2] &&= a(x,y) + b(x,y)\sin[\varphi(x,y)]
\end{aligned} \quad (13)$$

Equations (13) can be combined two by two to compute the tangent of $\varphi(x,y)$ independently of $a(x,y)$ and $b(x,y)$ as in Eq. (14). The output of the arctangent is a value between $-\pi/2$ and $+\pi/2$. It is possible to extend its output to $-\pi$ and $+\pi$ if the signs of the numerator and denominator are taken into consideration. However, that is not enough to determine $\varphi(x,y)$ uniquely. Only modulo 2π of $\varphi(x,y)$ can be determined, that corresponds to the angle in the first leap. It is needed to add $2\pi n$ to it,

where n is an unknown integer value. Since usually different points of the image have different n values, the notation $n(x,y)$ is more appropriate. Therefore, the phase values $\varphi(x,y)$ can be computed by Eq. (15). The module 2π of the fringe patterns of Figure 3 is represented in a gray scale in the left part of Figure 4. The sharp lines are the frontiers where the module 2π values jumps from $-\pi$ to $+\pi$ or vice-versa.

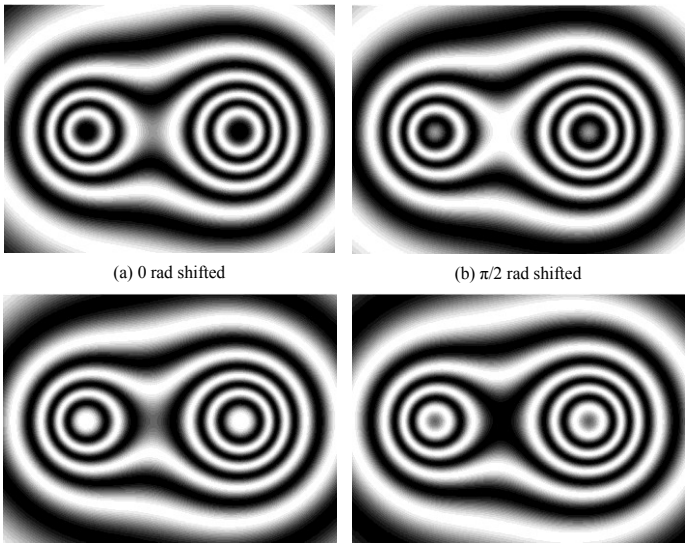

Figure 3. Four $\pi/2$ phase shifted images of the same fringe pattern.

$$\tan[\varphi(x,y)] = \frac{I_{3\pi/2}(x,y) - I_{\pi/2}(x,y)}{I_0(x,y) - I_\pi(x,y)} \tag{14}$$

$$\varphi(x,y) = \arctan\left[\frac{I_{3\pi/2}(x,y) - I_{\pi/2}(x,y)}{I_0(x,y) - I_\pi(x,y)}\right] + 2\pi n(x,y) \tag{15}$$

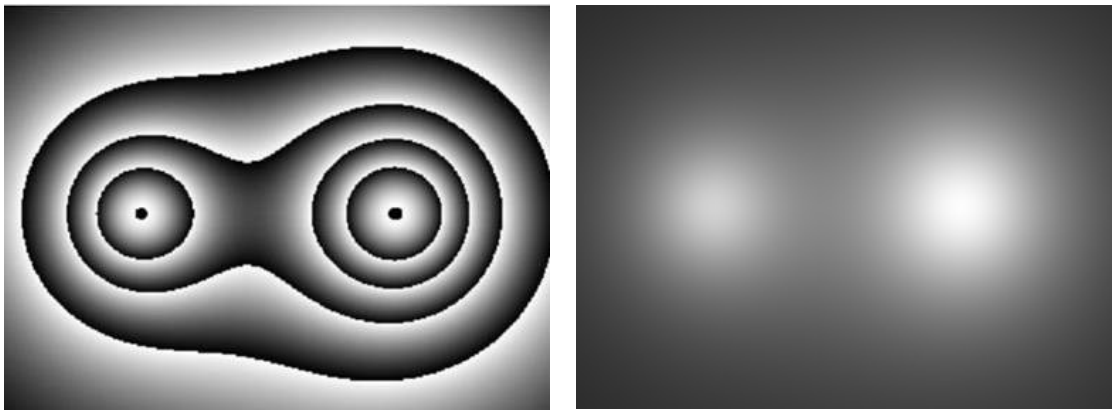

Figure 4. Module 2π of the fringe pattern of Figure 3 represented as a grey scale.

The least step to retrieve the phase values is the application of an algorithm known as *phase unwrapping*. This algorithm finds the set of constant integers $n(x, y)$ that are missing in Eq. (15). An output of the phase unwrapping algorithm is shown in the right part of Figure 4. Note that the phase jumps were removed and a continuous smooth surface was obtained. There are hundreds of different implementations of such algorithm. Most of them use spatial properties of neighbor pixels, assuming that the phase difference between any neighbor pixel can be greater than π radians. Some of them use temporal properties, what assumes that the phase difference for any given single point in the image does not change more than π radians for two consecutive frames. This very extensive topic will not be discussed here, however further information can be found in the good book wrote by Ghiglia and Pritt (please see the reference list).

1.2. Film Holography

The word *holography* comes from the combination of two Greek words: "holos" that means *whole* and "graphein" that means *write*. In essence, it is a method for recording and retrieving all information contained in a light wave: intensity and phase distributions. It was formally introduced in 1948 by the Hungarian scientist Dennis Gabor, which gave him the Nobel Prize for physics in 1971. Gabor's intentions were to improve image quality in electronic microscopy using a lens less process that did not work at that time for practical limitations. Only in the 1960s, after lasers were available, film holography become practical.

Holography is a combination of interference and diffraction to record and retrieve light waves. It uses laser light to print in a high resolution recording media the usually very fine interference patterns resulting of the interference of two coherent light waves: the *object wave* and the *reference wave*. After processing of the recording media, the fine interference pattern is known as *hologram*. Light coming from the reference wave only and going through the hologram is diffracted and three waves results. One of the diffracted components has the same phase of the object wave and its intensity is only modified by a scale factor. A viewer that looks into the reconstructed wave will see a three dimensional (3D) image of the object that is nearly impossible to be distinguished from the original object and is temped to touch the 3D image.

The first developments of holography were made in the early 1960s using high resolution photographic films and the reconstruction by optical means. Afterwards, in the late 1970s photothermoplastic films were made available as erasable recording media. Finally, in the middle 1990s the first applications of digital holography become practical using high resolution image sensors as recording media and numerical reconstruction of intensity and phase.

This text will start with film holography using high resolution films for recording the holograms and optical diffraction for reconstruction. Next, a section about holographic interferometry will be presented, as well experimental mechanics applications. Finally, the last section will introduce digital holography

1.2.1. Hologram Recording

Phase and intensity distribution of a light wave can be recorded in a high resolution photographic film H in the way represented in Figure 5. Light coming from a laser is split in two parts by the beam splitter BS. The part deflected by the beam splitter BS is directed to the object by mirror M1, is expanded by a lens L1 and illuminates the area of interest on the object. Every point of the object behaves like a spherical point source that emits light in all directions, including toward the film H. The summation of all point sources on the object surfaces forms the object wave $\mathbf{O}$. The object wave reaches the photographic film H. At the same time, the photographic film is exposed to a reference wave $\mathbf{R}$ that goes through the beam splitter BS, is reflected by mirror M2 and is expanded by lens L2 forming a spherical wave. The reference wave does not need to be a spherical or a plane wave; however spherical or plane waves are frequently used since they are easy to be produced. Since both object and reference waves come from the same laser source, they have the same frequency. In addition, if the optical path differences between the light rays that form the reference wave and the object waves are smaller than the coherence length of the laser, both waves interfere producing an interference fringe pattern stable in time. The interference fringe pattern is printed in the high resolution film. After photographic processing, the developed film is named *hologram*.

The high resolution photographic film that forms the hologram is a special one. Usually ordinary black and white films have a spatial resolution of about 100 to 150 lines per millimeter. Holographic films are usually made of silver halides, dichromated gelatins, photoresists or photo polymers and are frequently attached to a rigid glass plate. The spatial resolutions of holographic films are in the range from 3000 to 10000 lines per millimeter. This is an important property that limits the maximum angle between the interference and object waves. The interference fringe spacing d of two plane waves forming an angle α between them is computed by Eq. (16). For a wavelength of 633 nm and α = 1°, about 28 lines per millimeter are formed. For $\alpha = 10°$, this number increases to 275. For $\alpha = 30°$, they are 820 lines per millimeter.

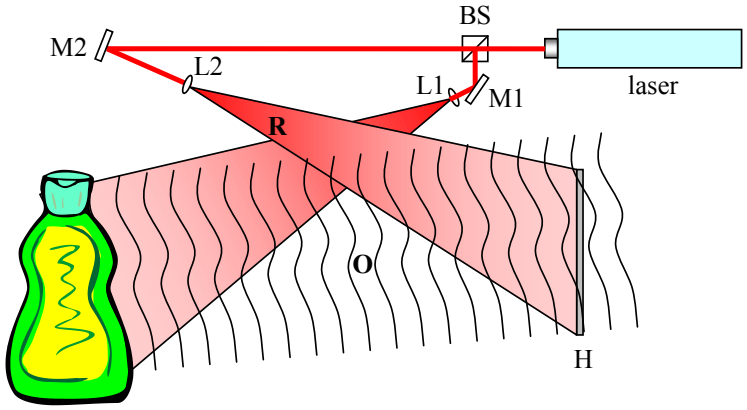

Figure 5. Recording of a hologram

$$d = \frac{\lambda}{2\sin(\alpha/2)} \tag{16}$$

It is necessary to keep the relative position of all optical elements and the object stable during the exposure time. Usually the arrangement of Figure 5 is setup on the surface of a vibration isolated optical bench. The maximum amount of tolerable relative motion is in the range of about $\lambda/4$.

The film is exposed to the intensity of the interference fringe patterns between the reference and the object waves. Omitting the time dependency of both waves, and packing all spatial dependency of the phase in $\varphi(\mathbf{r})$, a single function of $\mathbf{r}$, the reference and object waves are given in the complex form by Eq. (17). Here the explicit dependence of $\mathbf{r}$ is also omitted but only to make the equations shorter.

$$\begin{aligned} O(\mathbf{r}) &= O_0\, e^{i\varphi_O} \\ R(\mathbf{r}) &= R_0\, e^{i\varphi_R} \end{aligned} \tag{17}$$

The resulting intensity can be computed by:

$$\begin{aligned} I(\mathbf{r}) &= [O(\mathbf{r}) + R(\mathbf{r})][O^*(\mathbf{r}) + E^*(\mathbf{r})] \\ &= O_0^2 + R_0^2 + O_0 R_0 e^{i(\varphi_O + \varphi_R)} + O_0 R_0 e^{-i(\varphi_O + \varphi_R)} \end{aligned} \tag{18}$$

After been exposed to the intensity distribution given by Eq. (18), the photographic film is developed and is named *hologram*. It will become darker in the intensity maxima and more transparent in the minima regions. The response of the film is not perfectly linear, however it can be close enough to the linear behavior if the object to reference wave intensity ratio is closer to three Therefore, the *degree of transmittance* of the hologram, τ, is related to the resulting intensity by a linear equation like $\tau(\mathbf{r}) = \alpha + \beta.I(\mathbf{r})$. Finally, the degree of transmittance of the hologram can be computed by:

$$\tau = \alpha + \beta(O_0^2 + R_0^2 + O_0 R_0 e^{i(\varphi_O + \varphi_R)} + O_0 R_0 e^{-i(\varphi_O + \varphi_R)}) \tag{19}$$

Equation (19) is valid for a so called *amplitude hologram*, where darker and brighter areas of the hologram change locally the amplitude of a light wave that propagates through it. There are also *phase holograms*, where the film produces local phase retardations proportional to the resulting intensity of Eq. (18). That is possible after special chemical processing of a photographic film or is directly obtained using thermoplastic films.

1.2.2. Hologram Reconstruction

The object wave can be reconstructed from the hologram when it is exposed to the reference wave ***R***. A usual configuration is shown in Figure 6. After developing, the

hologram is replaced in the same place where it was exposed and it is illuminated only by the reference wave. Light that goes through the hologram is diffracted. One of the diffraction orders has the same phase distribution as the object wave and its intensity is proportional to the object wave.

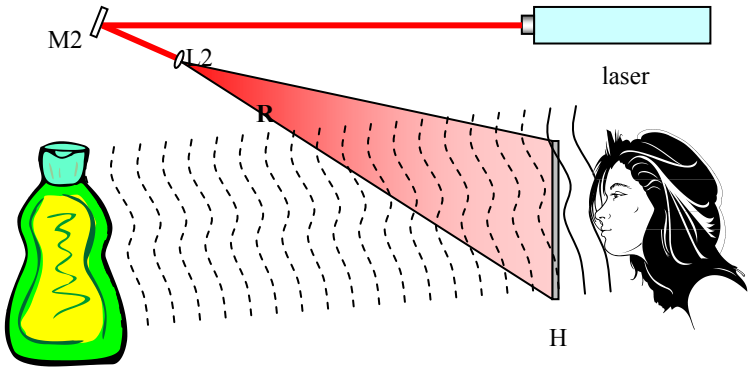

Figure 6. Light wave reconstruction from a hologram

The light wave that comes out from a hologram, $C(\mathbf{r})$, can be easily computed multiplying the incident light wave, $R(\mathbf{r})$, by the degree of transmittance of the hologram, given by Eq. (19):

$$C(\mathbf{r}) = \tau(\mathbf{r})R(\mathbf{r})$$

$$C(\mathbf{r}) = [\alpha + \beta(O_0^2 + R_0^2 + O_0R_0e^{i(\varphi_O+\varphi_R)} + O_0R_0e^{-i(\varphi_O+\varphi_R)})]R_0e^{-i\varphi_R}$$

$$C(\mathbf{r}) = \alpha R_0e^{-i\varphi_R} + \beta O_0^2R_0e^{-i\varphi_R} + R_0^2R_0e^{-i\varphi_R} + \beta O_0R_0^2e^{i\varphi_O} + \beta O_0R_0^2e^{-i(\varphi_O+2\varphi_R)}$$

That can be reorganized as:

$$C(r) = [\alpha + \beta(O_0^2 + R_0^2)]R_0e^{-i\varphi_R} + \beta O_0R_0^2e^{i\varphi_O} + \beta O_0R_0^2e^{-i(\varphi_O+2\varphi_R)} \qquad (20)$$

The first term of Eq. (20) has the same phase distribution of the reference wave φ_R. It corresponds to the undiffracted wave, or zero order diffraction term, that went through the hologram. The second term has the same phase distribution as the object wave φ_O and its amplitude corresponds to the object wave scaled by a factor of $\beta R_0{}^2$. Finally, the third term combines phase of both waves and forms a *conjugated image* of the object wave. The conjugate image of the object image is a converging one which can be focused on a screen, being named as *real image*.

Someone that is placed behind the hologram and is exposed to the second term will have the same sensation as to be exposed to the real object wave. A true virtual three dimensional (3D) image of the object is viewed. The quality of the reconstructed 3D image of the object is so good that it can not be distinguished from the original object itself.

-

-

Bibliography

[1] Butters, J. N. and Leendertz, J. A. (1971). Speckle pattern and holographic techniques in engineering metrology. Opt. Laser. Technol. 3, 26-30 . [This paper describes first applications of speckle methods]

[2] Jones, R. and Wykes, K. (1989). Holographic and speckle interferometry. Second edition, Cambridge University Press. [This book describes deeply the beginning of the use speckle methods]

[3] Erf, R. K. (1978). Speckle metrology. Academic Press New York. [This book describes main application of speckle methods]

[4] Ennos, A. E. (1984). Speckle Interferometry, in *Laser Speckle and Related Phenomena*, second edition. Dainty, J. C. editor. Springer-Verlag, Berlin. Pp. 203-253.

[5] Françon, M.(1978). *La granularité laser (Speckle)*. Second edition, Mason. Paris. [This book describes the speckle phenomenon in a deep way]

[6] Goodman, J. W. (1975). Statistical Properties of Laser Speckle Patterns. In *Laser Speckle and Related Phenomena*, Dainty J. C., editor, pages 9 – 75. Springer – Verlag, Berlin. [This chapter describes superficially speckle statistics]

[7] Fernández Doval, A. M. (1997). Una aproximación sistemática a la holografía-TV y desarrollo de nuevas técnicas para la cuantificación y el análisis de magnitudes dinámicas con periodicidad temporal. PhD thesis, Departamento de Física Aplicada, Universidad de Vigo, Vigo, Spain (in Spanish). [Author in his thesis performs a deep description of speckle methods to measure temporal phenomena]

[8] Lehmann, M. (2001). Speckle statistics in digital speckle metrology. In *Digital speckle pattern interferometry and related techniques*. Rastogi, P. K. editor. Wiley, Chichester. [This chapter describes deeply and enjoyably speckle statistics].

[9] Goodman, J. W. (1985). *Statistical optics*, Wiley, New York. [This book describes deeply speckle statistics]

[10] Burch, J. M. and Tokarski, J. M. (1968). "Production of multi-beam fringes from photographic scatters". *Opt. Acta*. 15, 101-111.

[11] Jones, R. and Wykes, C. (1983). *Holographic and speckle interferometry*, Cambridge University Press, Cambridge, 1983. [This book describes superficially first application of speckle and holography methods]

[12] Sirohi, R. S. (1991). *Selected papers on speckle metrology*, SPIE Milestone series, MS35, SPIE Optical Engineering Press, Washington, DC. [This book joins several works about speckle and its associated methods]

[13] Sirohi, R. S. (1993). *Speckle metrology*, Marcel Decker, New York. [This book joins several authors in order to show a wide view about speckle methods].

[14] Rastogi, P. K. (1998). Special Issue on Speckle Photography. *Opt. Lasers Eng*. 29 (2 and 3). [This special issue of OLEN shows a brief description of speckle photography associated techniques]

[15] Sjödahl, M. and Benckert, L. R. (1993). Electronic speckle photography: analysis of an algorithm giving the displacement with subpixel accuracy. *App. Opt.* 32, 2278-2284. [This paper describes deeply a particular algorithm used to speckle photography]

[16] Sjödahl, M. and Benckert, L. R. (1994). Systematic and random errors in electronic speckle photography. *App. Opt.* 33, 7461-7471. [This paper performs a deep study about error in speckle photography]

[17] Sjödahl, M. (1994). Electronic speckle photography: increased accuracy by nonintegral pixel shifting. *App. Opt*. 33, 6667-6673. [This paper describes deeply a particular algorithm used to speckle photography]

[18] Sjödahl, M. (2001). Digital speckle photography. In *Digital speckle pattern interferometry and related techniques*. Ratogi, P. K. Editor. John Wiley and Sons, Ltd. Chichester, 2001. [This chapter gives an adequate idea of speckle photography being appropriated for a first contact with this technique]

[19] Huntley, J. M. (1989). Speckle photography fringe analysis: assessment of current algorithms. *App. Opt*. 28, 4316-4322. [This paper performs a enjoyable evaluation of algorithms used in speckle photography]

[20] Malacara, D., Servín, M., and Malacara, Z. (1998). Interferogram analysis for optical testing. *Optical Engineering*. Marcel Dekker, New York. [This paper gives ideas about method used to optical measurement]

[21] Moore, A. J. and J. R. Tyrer. (1990). An electronic speckle pattern interferometer for complete in-plane measurement. *Meas. Sci. Tech*. 1, 1024-1030. [This paper presents applications of polarizing systems to measure in-plane displacements in several directions]

[22] Moore, A. J. and Tyrer, J. R. (1996). Two-dimensional strain measurement with ESPI. *Opt. Lasers Eng*. 24, 381-402. [This paper presents applications of polarizing systems to measure in-plane displacements in several directions]

[23] Albertazzi, A., Borges, M. R., and Kanda, C. (2000). A radial in-plane interferometer for residual stresses measurement using ESPI. In Proc. IX Int. Congress on Exp.Mech., pages 108-111. Society for Experimental Mechanics. [This paper describes deeply principles of radial interferometers]

[24] Viotti, M. R. and Kaufmann, G. H. (2004). Accuracy and sensitivity of a hole drilling and digital speckle pattern interferometry combined technique to measure residual stresses. *Opt. Lasers Eng.*, 41:297-305. [This paper describes a typical application of speckle methods with a traditional interferometer]

[25] Viotti, M. R., Suterio, R., Albertazzi, A., and Kaufmann, G. H. (2004). Residual stress measurement using a radial in-plane speckle interferometer and laser annealing: preliminary results. *Opt. Lasers Eng*., 42:71-84. [This paper describes a special application of the radial interferometer]

[26] Viotti M. R., Albertazzi A. Jr. and Kaufmann G. H. (2005). Measurement of residual stresses using local heating and a radial in-plane speckle interferometer. *Opt. Eng*., 093606-1. [This paper describes a special application of the radial interferometer]

[27] Albertazzi, A. (2006). Radial Metrology with ESPI, Radial metrology with electronic speckle pattern interferometry. *Journal Holography Speckle*, v. 3, p. 117-124. [This paper describes deeply radial applications]

[28] Ghiglia D. C., Pritt M. D. (1998). *Two-dimensional phase unwrapping. Theory, algorithms, and software*. Jon Wiley and Sons, Inc. New York. [This book can be considered as the Bible for developers of phase unwrapping algorithms]

Biographical Sketches

Armando Albertazzi Gonçalves Júnior: Prof. Armando Albertazzi G. Jr received his Dr. Eng. degree in Mechanical Engineering from the Federal University of Santa Catarina, Brazil, in 1989. He worked as a research associate at the Mechanical and Aerospace Engineering Department of the Illinois Institute of Technology in Chicago from 1989 to 1991. Currently he is a professor and director of the Metrology Laboratory of the Mechanical Engineering Department of this same university. His major research

interest is applied optical metrology for 3D shape, stresses and residual stresses measurement. He has graduated 28 masters and 11 Dr. Eng., all in the field of optical metrology and is author or co-author of about 120 papers, most of them published in proceedings of international conferences on optical metrology. In 2008 he was graded Fellow of the International Society of Optical Engineering - SPIE.

Matias Roberto Viotti: Matías R. Viotti his Dr. Eng. degree in Mechanical Engineering from the Universidad Nacional de Rosario, Argentina, in 2005. He worked as a research associated at Metrology Laboratory of the Mechanical Engineering Department from 2005 to 2007. He is currently a researcher of the Optical Metrology Division of the company Photonita Ltd . He has authored and coauthored more than 25 scientific papers published in refereed journals and proceedings of international conferences. His major research interests include electronic speckle pattern interferometry, the measurement of residual stresses and the development of coherent techniques for strain analysis and nondestructive testing. He is also a member of SPIE and OSA.